International Journal of Engineering

Journal Homepage: www.ije.ir

Natural frequency of Sandwich Beam Structures with Two Dimensional Functionally Graded Porous Layers Based on Novel Formulations

P. Mehdianfar, Y. Shabani, K. Khorshidi*

Department of Mechanical Engineering, Arak University, Arak, Iran

P A P E R I N F O

Paper history:
Received 04 February 2022
Received in revised form 16 July 2022
Accepted 24 July 2022

Keywords:
Vibration Analysis
Porous
Two-dimensional Functionally Graded Materials
Galerkin Method
Sandwich Beam

A B S T R A C T

This study presents an analytical solution for free vibration analysis of two-dimensional functionally graded (2D-FG) porous sandwich beams. The equations of motion for the beam were derived using Hamilton's principle, and then the Galerkin method was employed to solve the equations. The material properties of the sandwich beams vary with the thickness and length of each layer according to the power-law function. The mechanical properties gradually changed from aluminum to alumina as the metal and ceramic, respectively. The vibration analysis was investigated based on two new higher-order shear deformation beam theories (NHSDBTs). These two new theories do not need any shear correction factor and have fewer unknown variables than other higher order shear beam theories. The obtained natural frequencies for the three types of beams were compared with the results of the Timoshenko, first-order , and parabolic shear deformation beam theories. In addition, the effects of porosity, L/h, and FG power indexes along the thickness and length on the non-dimensional frequency of three special types of beams are presented and discussed. Furthermore, the mode shapes of the beam are depicted for various FG power indexes based on these new theories. By comparing the results of the two proposed theories with those of existing studies, the accuracy of the proposed theories was validated. Power-law indexes shifted the node point to the left and resonance will be accrued sooner than the non-FGM beam.

doi: *10.5829/ije.2022.35.11b.04*

1. INTRODUCTION

Functionally graded (FG) materials are usually formed by combining a certain volume ratio with ceramics and metals materials. These materials have been highly discussed among researchers because they include characteristics such as: heat-resistance, toughness, low volumetric mass and high strength. Sandwich structures are widely used in the aerospace, space, shipbuilding and construction industries due to their excellent electrical, thermal and mechanical properties. Research on the different aspects of FG beams has been conducted extensively in recent years [1-3]. Typically, functionally graded material is a compositional gradient but it can also be a microstructural gradient, for instance, porosity gradients. As far as the search for literature goes, a few studies were carried out on the mechanical actions of porous structures [4, 5].

The higher shear deformation theories (HSDT) support transverse shear effects, hence is appropriate for analysis of both moderately thick and thin plates and beams. Vibration behaviours of FG structures have been investigated in many studies. For example, in a study, the free vibration of simply supported functionally graded beams (FGs) whose material properties may be arbitrarily altered in thickness direction has been undertaken by Celebi et al. [6]. In a different work, Lei et al. [7]. examined a size-dependent model of beam to study vibration and bending of FG microbeams with simply supported boundary conditions based on the strain gradient elasticity theory and sinusoidal shear deformation theory. Ke et al. [8]. considered the non-linear free vibration of FG nanotube-reinforced composite beams by employing direct iterative and Ritz method based on the TBT and using von Karman type strain-displacement relationships. Researchers have used various numerical methods to analyze FG beam

*Corresponding Author Institutional Email: k-khorshidi@araku.ac.ir (K. Khorshidi)

vibrations. Free vibration of FGM layered beams under various boundary conditions through the use of finite element method were analyzed by Mashat et al. [9]. Recently, Faghidian [11-13] developed size-dependent elasticity theories such as the nonlocal modified gradient theory [10], the higher-order nonlocal gradient theory for analyzing the mechanical behavior of nanostructures. Shahba and Rajasekaran [14] calculate the longitudinal transverse frequencies of FGM beams applied the differential transform element method (DTEM) and differential quadrature element method (DQEM) of lower order. The vibrational analysis of composite beams is carried out in different studies [15, 16]. Shafiei et al. [17] employed the DQM to investigate vibration of 2D FG Timoshenko nano and micro beams with porosity. Kandil et al. [18] studied sandwich panels with various properties of face and core. They found decreasing thickness of concrete face wythes had a positive effect on strength/weight ratio. Singh and Sangle [19] were studied nonlinear static response of vertically oriented coupled wall with finite element method.

Based on the studies mentioned above, it can be noted that the studies vibration of two-dimensional functionally graded sandwich beams with porosity are very limited. For the first time, natural frequency analysis of the 2D-FG sandwich beams investigated based on two new higher order theories. Vibration analysis of two-dimensional functionally graded beams by considering the porosities that might occur inside the materials with gradient properties during manufacturing process is presented. Three types of sandwich beams were investigated in second section. In the first type, a single-layer 2D-FG porous beam is assumed. The second type is sandwich beam with 2D-FG core and pure metal/ceramic face sheet. FG layers have a smooth and gradual change in mechanical behaviour throughout their length and thickness. On the other hands, the third type we have two 2D-FG layers with porosity as faces and pure ceramic core. In present research, Alumina (Al_2O_3) and Aluminium (Al) are considered as ceramic and metal, respectively. Two new beam theories are introduced. results obtained with new higher shear deformation beam theories (NHSDBT1 and 2) show great convergence with Timoshenko (TBT), first-order (FSDBT), and parabolic (PSDBT) shear deformation beam theories. In this paper at first, formulations and types of beams, governing equation of motion and solving method are presented at end of section two. Then, accuracy of our two new higher order formulations is confirmed and the influence of porosity, L/h, shapes, and FG power indexes along thickness and length on non-dimensional natural frequencies on the beams are discussed in the last section. Also, natural frequencies with various beam theories are calculated and results are concluded. Both novels introduced theories are simple than some other higher beam theories because of fewer unknown variables as a result it helps to reduce the time of calculating. Also, one of the other advantages of these two new proposed distributions is that they don't need any shear correction factor and they satisfy free stress conditions at the top and bottom surfaces of the structure.

2. PROBLEM AND FORMULATION

2. 1. Numerical Simulation Procedure Consider a beam, as shown in Figure 1 with length L, width b, and thickness h, with the Cartesian coordinate system O (x y z), where the origin of coordinate system O is chosen at the left of the beam. The mechanical properties of the beam, such as Young's modulus E (x, z), shear modulus G (x, z), Poisson's modulus υ (x, z), and mass density ρ (x, z), with the material properties can vary along the length and thickness, as shown in Figure 1. In this study, three different types of 2D-FG beam models were considered: isotropic 2D-FG beam (Model I), sandwich beam with homogeneous faces and 2D-FG core (Model II), and sandwich beam with 2D-FG faces and homogeneous ceramic core (Model III).

The effective material properties (P) can be expressed using the rule of mixtures as follows:

$$P(x,z)=P_cR_c(x,z)+P_mR_m(x,z) \tag{1}$$

$$R_c(x,z)+R_m(x,z)=1 \tag{2}$$

where P_c and P_m are the epitomes of the mechanical properties. In addition, R_c and R_m are the volume fractions of ceramic and metal. The effective material properties of the porosity are defined as follows [20]:

$$P(x,z)=(P_c-P_m)R_c+P_m-\left(\frac{\eta}{2}(P_c+P_m)\right) \tag{3}$$

where η is porosity volume fraction.

2. 1. 1. Model Ⅰ: Isotropic 2D-FG Beam The first beam Model was graded from the metal at the lower left corner edge to the ceramic at the top right corner edge (Figure 2). The volume fraction of the ceramic material is given by Şimşek [21]:

$$R_c(x,z)=\left(\frac{x}{L}\right)^{k_x}\left(\frac{z}{h}+\frac{1}{2}\right)^{k_z} \tag{4}$$

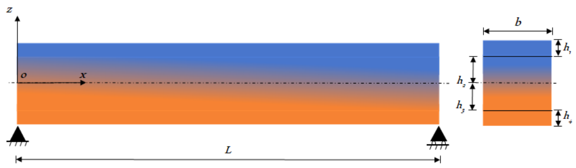

Figure 1. Geometry of 2D-FG beam and cross section

Figure 2. Isotropic 2D-FG beam, Model I

k_x and k_z are the power laws of the beam, which have certain properties in the length and thickness directions.

2. 1. 2. Model Ⅱ: Homogeneous Faces and 2D-FG Core

In this Model, the core layer of the sandwich beam is similar to that of Model I, and the bottom and top faces are made of pure metal and pure ceramic as shown in Figure 3. The volume fraction of the ceramic for the second Model is given by the following expression:

$$R_c(x,z)=\begin{Bmatrix} 1 & h_2<z<\dfrac{h}{2} \\ \left(\dfrac{x}{L}\right)^{k_x}\left(\dfrac{\mathrm{h}_2-\mathrm{z}}{\mathrm{h}_2-\mathrm{h}_3}\right)^{k_z} & h_3<z<h_2 \\ 0 & -\dfrac{h}{2}<z<h_3 \end{Bmatrix} \tag{5}$$

2. 1. 3. Model Ⅲ: 2D-FG Faces and Ceramic Core

In Model III, the two 2D-FG skins covered a homogeneous pure ceramic layer (Figure 4). In this case, the volume fraction of the ceramic constituent $R_c(x, z)$ is given as follows:

$$R_c(x,z)=\begin{Bmatrix} \left(\dfrac{x}{L}\right)^{k_x}\left(\dfrac{(\mathrm{h}_2+h_1)-z}{h_1}\right)^{k_z} & h_2<z<\dfrac{h}{2} \\ 1 & h_3<z<h_2 \\ \left(\dfrac{x}{L}\right)^{k_x}\left(\dfrac{(\mathrm{h}_3+h_4)-z}{h_4}\right)^{k_z} & -\dfrac{h}{2}<z<h_3 \end{Bmatrix} \tag{6}$$

The variation of the volume fraction of the ceramic (R_c) through the beam thickness and length for all three Models with respect to k_x and k_z is plotted in Figure 5.

2. 2. Numerical Simulation Procedure

The displacement field for the present shear deformation beam theories, are given by Equation (7):

Figure 3. Sandwich beam with homogeneous faces and a 2D-FG core, Model II

Figure 4. Sandwich beam with 2D-FG faces and homogeneous ceramic core, Model III

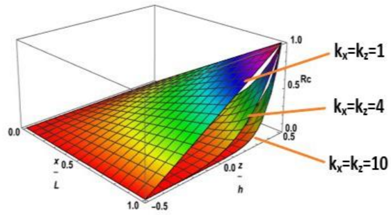

(a) Model I

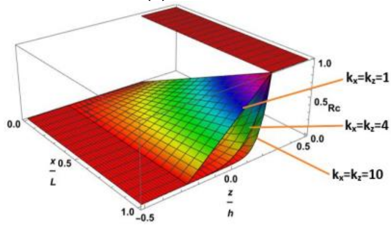

(b) Model II

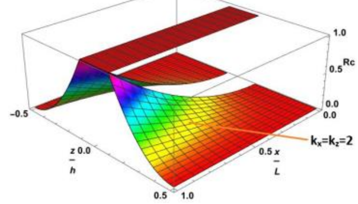

(c) Model Ⅲ

Figure 5. Variation of volume fraction of the ceramic (R_c) through the beam thickness and length according to power-law indexes

$$u_x(x,z)=u(x)-g(z)\frac{\partial w(x)}{\partial x}+f(z)\varphi(x) \tag{7a}$$

$$u_z(x,z)=w(x) \tag{7b}$$

where u(x) and w(x) represent the axial and transverse displacements for the mid access, respectively, and φ is the rotation of the cross sections. g(z) and f(z) are shape functions that differ based on the theory under consideration, as listed in Table 1. In this study, two new

TABLE 1. Various theories for Modelling the structure

Theories	g(z)	f(z)
TBT [22]	0	z
FSDBT [23]	z	z
PSDBT [24]	z	$z\left(1-\dfrac{4z^2}{3h^2}\right)$
NHSDBT1	z	$z\left(\dfrac{4}{h}-\dfrac{16z^2}{3h^3}\right)$
NHSDBT2	z	$z\left(\dfrac{1}{h}-\dfrac{2z^2}{h^3}+\dfrac{8z^4}{5h^5}\right)$

higher-order shear deformation theories, NHSDBT1 and NHSDBT2, were introduced for the first time.

By assuming infinitesimal deformations, strain-displacement relations are [25]:

$$\varepsilon_{xx} = \frac{\partial u(x)}{\partial x} - g(z)\frac{\partial^2 w(x)}{\partial x^2} + f(z)\frac{\partial \varphi(x)}{\partial x} \tag{8a}$$

$$\gamma_{xz} = -\frac{\partial g(z)}{\partial z}\frac{\partial w(x)}{\partial x} + \frac{\partial f(z)}{\partial z}\varphi(x) + \frac{\partial w(x)}{\partial x} \tag{8b}$$

The stress-strain relations by using Hook's law defined. The Hamilton's principle is employed to extract equations of motion [26]:

$$\int_0^t (\delta U - \delta T)dt = 0 \tag{9}$$

where U and T are the strain and kinetic energies of the beam, respectively. δ denotes the variation operator. The strain energy of the beam (U) is calculated as follows [27]:

$$U = \frac{1}{2}\int_V \sigma_{ij}\varepsilon_{ij}dV = \frac{1}{2}\int_V (\sigma_{xx}\varepsilon_{xx} + \tau_{xz}\gamma_{xx})dV \tag{10}$$

Finally, the variation of strain energy with respect to u(x), w(x) and $\varphi(x)$ is shown as follows:

$$\delta U = \frac{1}{2}\int_A \left[-\delta u\frac{\partial \mathrm{A_{xx}}}{\partial x} - \delta w\left(\frac{\partial^2 \mathrm{B_{xx}}}{\partial x^2} - \frac{\partial \mathrm{S_{xz}}}{\partial x} + \frac{\partial \mathrm{A_{xz}}}{\partial x}\right) - \delta\varphi\left(\frac{\partial \mathrm{D_{xx}}}{\partial x} - \mathrm{T_{xz}}\right)\right]dA \tag{11}$$

Where A_{xx}, A_{xz}, B_{xx}, D_{xx}, S_{xz} and T_{xz} are defined by:

$$(\mathrm{A_{xx}}, \mathrm{A_{xz}}) = -\int_{-h/2}^{h/2}(\sigma_{xx}, \tau_{xz})\mathrm{dz} \tag{12a}$$

$$(\mathrm{B_{xx}}, \mathrm{D_{xx}}) = \int_{-h/2}^{h/2}(\mathrm{g(z)}, \mathrm{f(z)})\,\sigma_{xx}dz \tag{12b}$$

$$(\mathrm{S_{xz}}, \mathrm{T_{xz}}) = \int_{-h/2}^{h/2}\left(\frac{\partial \mathrm{g(z)}}{\partial \mathrm{z}}, \frac{\partial \mathrm{f(z)}}{\partial \mathrm{z}}\right)\tau_{xz}dz \tag{12c}$$

The kinetic energy is obtained as follows [28]:

$$T = \frac{1}{2}\int_V \rho\left[\dot{u}_x^{\,2} + \dot{u}_z^{\,2}\right]dV \tag{13}$$

The inertia coefficients are defined as Equation (14) [25]

$$(\mathrm{I_1}, \mathrm{I_2}, \mathrm{I_3}, \mathrm{I_4}, \mathrm{I_5}, \mathrm{I_6}) = -\int_{-h/2}^{h/2}\rho\big(1, g(z), f(z), \\ g(z)f(z), g(z)^2, f(z)^2\big)dz \tag{14}$$

Finally, the total variation of the kinetic energy associated with the sandwich beam in the integral form is:

$$\delta T = \frac{1}{2}\int_A \Big[\Big(-\mathrm{I_1}\ddot{u} + \mathrm{I_2}\frac{\partial \ddot{w}}{\partial x} - \mathrm{I_3}\ddot{\varphi}\Big)\delta u + \Big(-\mathrm{I_3}\ddot{u} + \mathrm{I_4}\frac{\partial \ddot{w}}{\partial x} - \mathrm{I_6}\ddot{\varphi}\Big)\delta\varphi \\ -\Big(\mathrm{I_2}\frac{\partial \ddot{u}}{\partial x} - \mathrm{I_5}\frac{\partial^2 \ddot{w}}{\partial x^2} + \mathrm{I_4}\frac{\partial \ddot{\varphi}}{\partial x} - \mathrm{I_1}\ddot{w}\Big)\delta w\Big]dA \tag{15}$$

By substituting the strain energy Equation (11) and kinetic energy Equation (15) into Hamilton's principal, Equation (9), equations of motion may be expressed as Equation (16).

$$\delta u : \frac{\partial \mathrm{A_{xx}}}{\partial x} = \mathrm{I_1}\ddot{u} - \mathrm{I_2}\frac{\partial \ddot{w}}{\partial x} + \mathrm{I_3}\ddot{\varphi} \tag{16a}$$

$$\delta w : \frac{\partial^2 \mathrm{B_{xx}}}{\partial x^2} - \frac{\partial \mathrm{S_{xz}}}{\partial x} + \frac{\partial \mathrm{A_{xz}}}{\partial x} \\ = \mathrm{I_2}\frac{\partial \ddot{u}}{\partial x} - \mathrm{I_5}\frac{\partial^2 \ddot{w}}{\partial x^2} + \mathrm{I_4}\frac{\partial \ddot{\varphi}}{\partial x} + \mathrm{I_1}\ddot{w} \tag{16b}$$

$$\delta\varphi : \frac{\partial \mathrm{D_{xx}}}{\partial x} - \mathrm{T_{xz}} = \mathrm{I_3}\ddot{u} - \mathrm{I_4}\frac{\partial \ddot{w}}{\partial x} + \mathrm{I_6}\ddot{\varphi} \tag{16c}$$

2. 3. Analytical Solution To obtain the theoretical solution, the Galerkin method is considered. According to this method, the displacements functions u(x, t), w(x, t) and $\varphi(x,t)$ are assumed as follows [28, 29]:

$$u(x,t) = \sum_{m=1}^{K}\left[(L - x)^{q_0}\, x^{p_0} x^{m-1}\bar{u}_m\right]e^{iwt} \tag{17a}$$

$$w(x,t) = \sum_{n=1}^{K}\left[(L - x)^{q_0}\, x^{p_0} x^{n-1}\bar{w}_n\right]e^{iwt} \tag{17b}$$

$$\varphi(x,t) = \sum_{j=1}^{K}\left[(L - x)^{q_0}\, x^{p_0} x^{j-1}\bar{\varphi}_j\right]e^{iwt} \tag{17c}$$

where $\bar{u}_m$, $\bar{w}_n$ and $\bar{\varphi}_j$ are unknown coefficients which will be determine. i = $\sqrt{-1}$, K denote the order of series and ω is the natural frequency. These functions satisfy the fully clamped boundary conditions. Free vibration analysis of the bi-dimensional functionally graded sandwich beam can be computed from Equation (18) [30]:

$$\left\{[K] - \omega^2[M]\right\}\{\lambda\} = 0 \tag{18}$$

where, [M] and [K] are global mass and stiffness matrix, also ω and $\{\lambda\}$ are natural frequency of the beam and unknown coefficients, respectively.

3. NUMERICAL RESULTS AND DISCUSSION

In this section, the free vibration of three types of 2D-FG porous sandwich beam concerning porosity coefficients (η) for clamped-clamped boundary condition are studied and discussed. 2D-FG sandwich beam has various shapes, including (1-8-1), (1-1-1), (2-1-2) and (1-2-1). The first, second and third element indicates the thickness ratio of the top, core and bottom layer, respectively. Functionally graded material composed of mixture of alumina and aluminum as ceramic and metal, respectively with the material. Their properties are given in Table 2. The influence of different slenderness ratios, L/h = 5, 10, 15 and 20 for various theories, contains two new theories on the non-dimensional natural frequency are investigated. The shear correction factor for TBT and FSDBT theories is considered as k_s = 5/6 and for other theories are taken as k_s = 1.

The dimensionless fundamental frequency is defined as Equation (19) [31]:

$$\bar{\varpi} = \omega \frac{L^2}{h} \sqrt{\frac{12\rho_c}{E_c}} \tag{19}$$

where L, h are total length and thickness of the sandwich beam, moreover ρ_C, E_C are density and Young's modulus of the middle layer of the sandwich beam. In this research, the results are calculated for different power-law indexes between 0 to 10 and porosity coefficients are taken as η = 0, 0.1, and 0.2 in various displacements theories. The total thickness of beam (h) is constant and it is 0.1 m in all third Models I, II and III. The width of beam (b) considers as 0.1 m and the function indexes (p_0 and q_0), are taken as 2 to satisfy the clamped-clamped boundary condition. Validation of our formulation and the results are obtained and compared with the results reported in literature [25]. The material properties in Table 3 are used for this purpose. A flowchart of the configuration of the research paper is presented in Figure 6.

The distribution of transverse shear stress along the thickness of the structure for FSDBT, PSDBT, and two present introduced theories are illustrated in Figure 7. The modified shear deformation theory satisfies free stress conditions at z = -h/2 and the z = h/2 surfaces of the beam. In Table 4, the first frequency of FG porous-less beam with L/h = 10 for Model I based on the Galerkin method and clamped-clamped support condition for three different power-law indexes are

TABLE 2. Properties of materials

Materials	Elasticity module (E)	Mass density (ρ)	Poisson's ratio (υ)
Alumina	380	3965	0.23
Aluminium	70	2700	0.23

TABLE 3. Properties of materials reported by Elmeiche et al. [25]

Materials	Elasticity module (E)	Mass density (ρ)	Poisson's ratio (υ)
Alumina	380	3800	0.23
Aluminium	70	2700	0.23

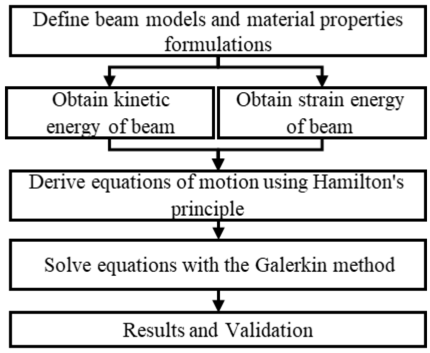

Figure 6. Research methodology flowchart

calculated. It is clear the present non-dimensional frequency values are in good agreement with the reference.

Moreover, the accuracy of our results and our new formulation is verified by comparison with the exact solution study for the non-dimensional frequencies of the FG beams [32]. The results are presented in Table 5 by assuming Bouamama et.al. material properties with L/h = 10, results show that our theories have high accuracy as proven by the good agreement between the results in all three first frequencies. The percentage below each value in Tables 4 and 5 represents the difference with the corresponding results obtained from references.

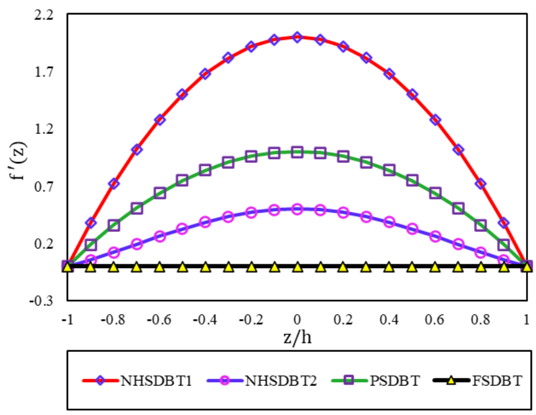

Figure 7. A comparison of transverse shear stress distributions of the beam based on various theories

TABLE 4. Comparison of the results of $\bar{\varpi}$ with Elmeiche et al. [25]

	k_w = 5		k_w = 10	
	FSDBT	**PSDBT**	**FSDBT**	**PSDBT**
Elmeiche et al [25]	14.2348	14.0866	13.6883	13.5237
Present	14.2380	14.1021	13.6966	13.5534
	-0.02%	-0.1%	-0.06%	-0.2%

TABLE 5. Comparison of the results with Mohamed et al. [32]

	ω_1	ω_2
NHSDBT1	21.3931 (4.3%)	58.3604 (5.37%)
NHSDBT2	21.4001 (4.3%)	58.3877 (5.32%)
Mohamed et al.[32]	22.3730	61.6730

In Table 6 natural frequencies of first type 2D-FG considered beam are calculated for all FSDBT, PSDBT, NHSDBT1 and NHSDBT2.

To show the accuracy of results of our two new theories for thick beam, we investigate natural frequencies of the 2D-FG beam in Table 7.

Fixed coefficients and their reduction rates in these two theories are different from other theories, hence this difference causes a change in the transverse shear strain. The results express a convergent by using these two new theories. According to this table, there is a bit different among the results obtained from various shear deformation theories. These differences are due to the fact that, function f(z) have different expansions through the thickness in various theories. It is worth to mention that every extra power in the expansion of function f(z) through the thickness of the structure includes additional unknown variables in those theories. Additionally, physical interpretation of these unknown variables are difficult [33]. Thus, it is better to use such distributions that are simpler with acceptable accuracy. Although two new proposed theories are simpler than other modified shear deformation theory, they are nearly identical in accuracy.

Figure 8, display the non-dimensional frequency (ω) of the 2D-FG porous beam of Model I for various values of power-law indexes (k_x and k_z). These figures are calculated based on new higher shear deformation theory (NHSDBT2) by assuming porosity volume fraction (η) and slenderness ratios (L/h) as 0.1 and 10. It is clear from the figure that the value of natural frequency decreases with increasing FG power-law indexes (k_x and k_z). This is because of the decrease in modulus of elasticity. Also, the flexibility of the sandwich beam increases while the power-law indexes increase. The first line (k_x=0) shows dimensionless frequencies for the one-dimensional FG beams, whereas other lines show the natural frequencies of the 2D-FG beams. It is clear that when the beam change to 2D-FG, the amount of non-dimensional frequencies will decrease.

In Figure 9, the effect of porosity on the natural frequency for NHSDBT1 and NHSDBT2 are illustrated. It is clear that porosity is not a significant parameter for frequency in the low amount of power-law index ($k_z < 2$). As the porosity increases, the rigidity of the beam decreases, which reduces the stiffness. Decreasing the stiffness, reduces the natural frequency value. In Figure. 10, two first modes of the natural frequency of 2D-FG sandwich beam respected to different slenderness ratios (L/h = 5, 10, 15 and 20) are compared. As the numerical value of the porosity parameter increases, we see more effectiveness of graded parameters

TABLE 6. Comparison of the results of $\bar{\omega}$ based on various theories for type 1, L/h = 10, k_x = 0 and η = 0

Theories	$k_z = 0$	$k_z = 1$	$k_z = 5$	$k_z = 10$
FSDBT	21.1695	16.5043	14.2380	13.6966
PSDBT	21.1690	16.5042	14.1021	13.5534
NHSDBT1	21.1618	16.5051	14.1027	13.5504
NHSDBT2	21.1791	16.5150	14.0906	13.5551

TABLE 7. Comparison of the results of $\bar{\omega}$ based on various theories for type 1, L/h = 5, k_x = 0 and η = 0

Theories	$k_z = 0$	$k_z = 1$	$k_z = 2$	$k_z = 6$	$k_z = 10$
FSDBT	18.538	14.665	13.380	12.250	11.800
PSDBT	18.559	14.680	13.297	11.899	11.468
NHSDBT1	18.559	14.677	13.297	11.898	11.470
NHSDBT2	18.590	14.703	13.309	11.888	11.480

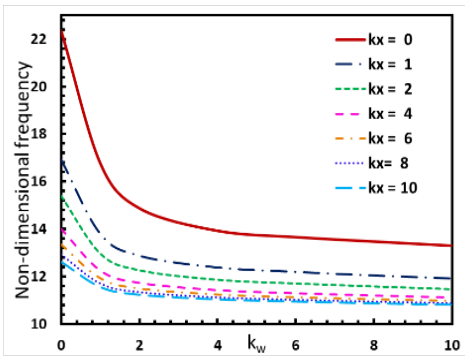

Figure 8. $\bar{\omega}$ of 2D-FG porous beam for various k_x and k_z based on NHSDBT2 theory (L/h = 10, η = 0.1 and Model I)

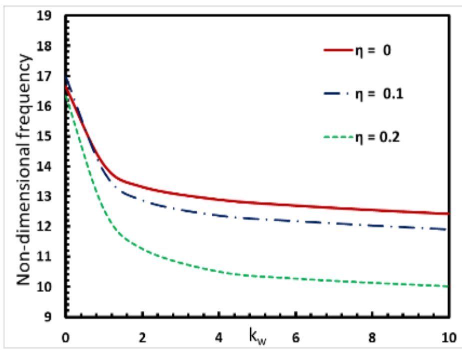

Figure 9. $\bar{\omega}$ of 2D-FG porous beam for various k_z and η, based on NHSDBT1 (L/h = 10, k_x = 1 and Model I)

As shown in Figure 10, L/h = 5 has more effect on frequencies in comparison with other slenderness ratios. In another word, free vibration frequencies decrease with decreasing value of L/h. Reducing the length to a constant thickness reduces the bending moment, which reduces the strain energy, which in turn reduces the natural frequency value. It is good to mention that, the decrement is higher for the second mode. It can be pointed out that slenderness ratios (L/h) effects become more prominent in smaller values on the natural frequencies of the beam.

To verify the accuracy of the two newly presented theories (NHSDBT1 and NHSDBT2), Figure 11 is plotted. A good agreement can be observed between the reported results. Our two new theories and parabolic shear deformation formulation come up with close results for Model I.

Figure 12 indicates that non-dimensional natural frequencies for Model II of the 2D-FG porous sandwich beam have good agreement with different theories. The effect of core thickness on the natural frequency for Model II is illustrated. In this figure, it can be observed 1-8-1 shape determine a larger range of natural frequency than other shapes. This is due to the ratio of the thickness of the core layer, which has no dependency on FG is larger than other shapes. In this Model specially, results of PSDBT always coincide with our two new higher shear deformation beam theories. Due to the graded properties of the beam, the natural frequencies change gradually, which starts from the metal phase and leads to the ceramic. For this reason, the values of the frequencies in the presented graphs have a downward trend.

Like Model II, results in Figure 13 shows great accuracy between theories for Model III, which demonstrates the validity of the new theories. On the other hand, in this figure, the 1-8-1 shape has the smallest range of natural frequencies variation and the 2-1-2 shape has the largest variation range among shapes. This is because FG face sheets are thicker in the 2-1-2 shapes compared to other shapes and the variation in the properties of FG material, affects the frequencies. Generally, amount of frequencies in 1-8-1 shape are higher than the others.

In Figure 14, dimensionless frequencies of the beam are graphed for assumptions of L/h = 10, η = 0.1 and k_x = 1 based on NHSDBT2. It is noteworthy that, the effect of FG layers on the natural frequencies of the 2D-FG beam is significant for variable k_z. Consequently, the 1-8-1 shape in Model II (Figure. 14(a)) and the 2-1-2 shape in Model III (Figure 14(b)) had most affected by the power-law index of functionally graded material, compared to the other shapes in each Model. The stiffness of FG beams will decrease as the power-law index is increased for all shapes types because FG material went to have more ceramic volume. Also, by

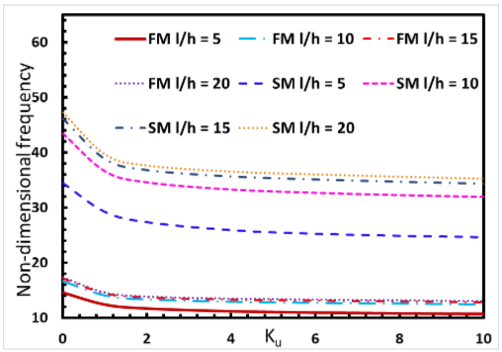

Figure 10. First and Second modes of $\overline{\omega}$ of 2D-FG porous beam respected to L/h, based on NHSDBT1 (η = 0, k_x = 1 and Model I)

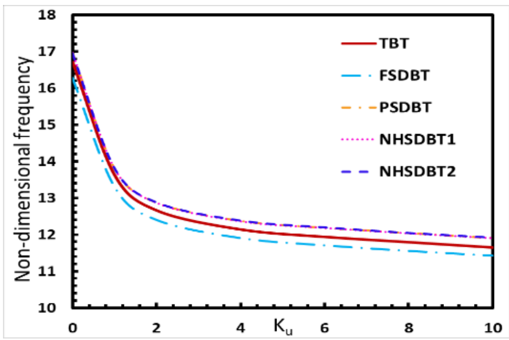

Figure 11. Comparison of $\overline{\omega}$ of 2D-FG porous based on different theories (η = 0.1, k_x = 1 and Model I)

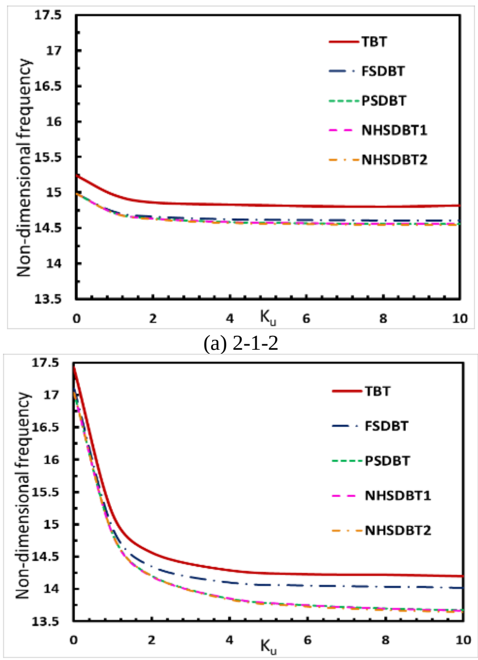

Figure 12. Comparison of $\overline{\omega}$ for various k_z and theories (L/h = 10, k_x = 1, η = 0.1 and Model II)

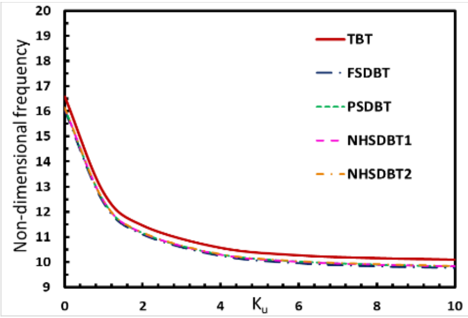

(a) 2-1-2

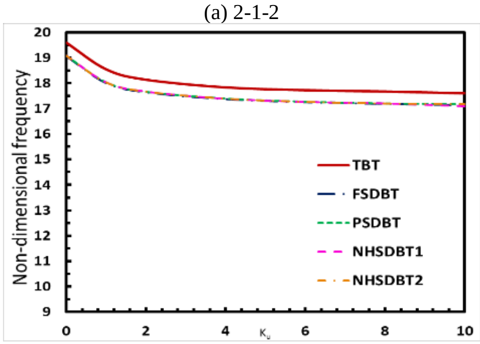

(b) 1-8-1

Figure 13. Comparison of ϖ for various k_z and theories (L/h = 10, k_x = 1, η = 0.1 and Model III)

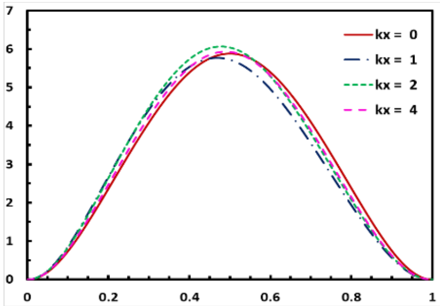

(a) First mode shape (×10⁻⁵)

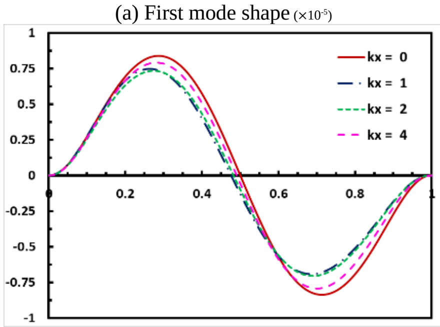

(b) Second mode shape (×10⁻⁵)

Figure 15. The first two mode shape of 2D-FG beam for Model I, based on NHSDBT1 (L/h = 10 and k_z = 1)

checking the results in model two, it is possible to achieve a unique natural frequency with various shapes. this phenomenon provides a state to use in reality. In Figure 15, based on our new theory (NHSDBT1) the first and second mode shapes of two dimensional functionally graded beam investigated. A fully clamped beam with L/h = 10 and k_z = 1 for various k_x based on Model I is chosen.

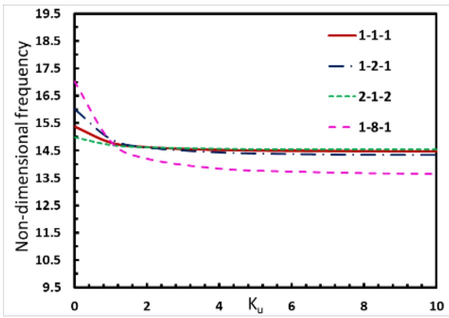

(a) Model II

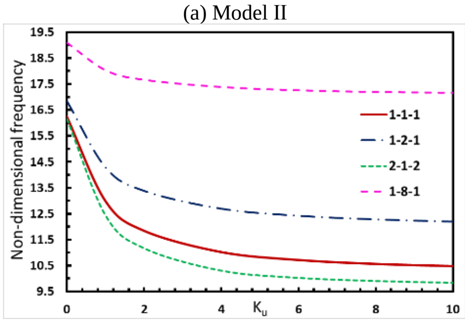

(b) Model III

Figure 14. ϖ of 2D-FG porous beam for various k_z and shapes, based on NHSDBT2 (L/h = 10, k_x = 1, and η = 0.1)

4. CONCLUSION

In this paper, two new higher order shear deformation beam theories (NHSDBT 1 and 2) to obtain non-dimensional frequencies of 2D-FG porous sandwich beams are introduced. Effect of different shapes, porosity (η), slenderness ratios (L/h) and power-law indexes in both axial and thickness directions (k_x and k_z) on natural frequencies of the 2D-FG porous beam in three different beam Models, based on various theories (TBT, FSDBT, PSDBT, NHSDBT 1 and 2) for clamped-clamped boundary condition are investigated. The higher order governing equations are derived by using Hamilton's principle. In the following, the Galerkin method is employed to solve them. The effect of power-law indexes on shape modes is illustrated. The presented theories are validated for the free vibration of beams. The major results of this paper are briefly explained below:

- By implementing the presented two new theories, a good agreement was obtained. The results indicate that the accuracy of the NHSDBT1 and NHSDBT2 are close to other order shear deformation beam theories although using the presented theories are easier than them.
- There are some parameters that will rise the amounts of natural frequencies by increasing them.

The slenderness ratio (L/h) is one of them, whereas the power-law indexes (k_x and k_z) and porosity volume fraction (η) show an indirect relation with frequencies. Frequencies are more sensitive to porosity in high-value power-law indexes.

- It is noteworthy that, the effect of FG layers on the natural frequencies of the 2D-FG beam is significant for variables k_x and k_z. Consequently, by increasing thickness of the functionally graded layer in each shape
- Generally, power-law indexes shifted the node point to the left and resonance will be accrued sooner than the non-FGM beam.

5. REFERENCES

1. Bakhshi Khaniki, H., Hosseini Hashemi, S. and Bakhshi Khaniki, H., "Free vibration analysis of functionally graded materials non-uniform beams", ***International Journal of Engineering, Transactions C: Aspects***, Vol. 29, No. 12, (2016), 1734-1740. doi: 10.5829/idosi.ije.2016.29.12c.12.
2. Sherafatnia, K., Farrahi, G.H. and Faghidian, S.A., "Analytic approach to free vibration and buckling analysis of functionally graded beams with edge cracks using four engineering beam theories", ***International Journal of Engineering, Transactions C: Aspects***, Vol. 27, No. 6, (2014), 979-990. doi: 10.5829/idosi.ije.2014.27.06c.17.
3. El Khouddar, Y., Adri, A., Outassafte, O., Rifai, S. and Benamer, R., "Non-linear forced vibration analysis of piezoelectric functionally graded beams in thermal environment", ***International Journal of Engineering, Transactions B: Applications***, Vol. 34, No. 11, (2021), 2387-2397. doi: 10.5829/ije.2021.34.11b.02.
4. Amoozgar, M. and Gelman, L., "Vibration analysis of rotating porous functionally graded material beams using exact formulation", ***Journal of Vibration and Control***, (2019), 10775463211027883. doi: 10.1177/10775463211027883.
5. Hadji, L., Bernard, F., Safa, A. and Tounsi, A., "Bending and free vibration analysis for fgm plates containing various distribution shape of porosity", ***Advances in Materials Research***, Vol. 10, No. 2, (2021), 115-135. doi: 10.12989/AMR.2021.10.2.115.
6. Celebi, K., Yarimpabuc, D. and Tutuncu, N., "Free vibration analysis of functionally graded beams using complementary functions method", ***Archive of Applied Mechanics***, Vol. 88, No. 5, (2018), 729-739. doi: 10.1007/s00419-017-1338-6.
7. Lei, J., He, Y., bo, Z., Gan, Z. and Zeng, P., "Bending and vibration of functionally graded sinusoidal microbeams based on the strain gradient elasticity theory", ***International Journal of Engineering Science***, Vol. 72, (2013), 36–52. doi: 10.1016/j.ijengsci.2013.06.012.
8. Ke, L.-L., Yang, J. and Kitipornchai, S., "Nonlinear free vibration of functionally graded carbon nanotube-reinforced composite beams", ***Composite Structures***, Vol. 92, (2010), 676-683. doi: 10.1016/j.compstruct.2009.09.024.
9. Mashat, D.S., Carrera, E., Zenkour, A.M., Al Khateeb, S.A. and Filippi, M., "Free vibration of fgm layered beams by various theories and finite elements", ***Composites Part B: Engineering***, Vol. 59, (2014), 269-278. doi: 10.1016/j.compositesb.2013.12.008.
10. Faghidian, S.A., "Flexure mechanics of nonlocal modified gradient nano-beams", ***Journal of Computational Design and Engineering***, Vol. 8, No. 3, (2021), 949-959. doi: 10.1093/jcde/qwab027.
11. Faghidian, S.A., Żur, K.K. and Reddy, J.N., "A mixed variational framework for higher-order unified gradient elasticity", ***International Journal of Engineering Science***, Vol. 170, (2022), 103603. doi: 10.1016/j.ijengsci.2021.103603.
12. Faghidian, S.A., "Higher order mixture nonlocal gradient theory of wave propagation", ***Mathematical Methods in the Applied Sciences***, (2020). doi: 10.1002/mma.6885.
13. Faghidian, S.A., "Two-phase local/nonlocal gradient mechanics of elastic torsion", ***Mathematical Methods in the Applied Sciences***, Vol. n/a, No. n/a, (2020). doi: 10.1002/mma.6877.
14. Shahba, A. and Rajasekaran, S., "Free vibration and stability of tapered euler–bernoulli beams made of axially functionally graded materials", ***Applied Mathematical Modelling***, Vol. 36, No. 7, (2012), 3094-3111. doi: 10.1016/j.apm.2011.09.073.
15. Wang, Y., Xie, K.-j., Fu, T. and Shi, C., "Vibration response of a functionally graded graphene nanoplatelet reinforced composite beam under two successive moving masses", ***Composite Structures***, (2019). doi: 10.1016/j.compstruct.2018.11.014.
16. Xu, J., Yang, Z., Yang, J. and Li, Y., "Free vibration analysis of rotating fg-cnt reinforced composite beams in thermal environments with general boundary conditions", ***Aerospace Science and Technology***, Vol. 118, (2021), 107030. doi: 10.1016/j.ast.2021.107030.
17. Shafiei, N., Mirjavadi, S.S., MohaselAfshari, B., Rabby, S. and Kazemi, M., "Vibration of two-dimensional imperfect functionally graded (2d-fg) porous nano-/micro-beams", ***Computer Methods in Applied Mechanics and Engineering***, Vol. 322, (2017), 615-632. doi: 10.1016/j.cma.2017.05.007.
18. Kandil, M., Abdelraheem, A., Mahdy, M. and Tahwia, A., "Effect of changing properties of wythes in precast structural sandwich panels", ***Civil Engineering Journal***, Vol. 6, (2020), 1765-1778. doi: 10.28991/cej-2020-03091581.
19. Singh, V. and Sangle, K., "Analysis of vertically oriented coupled shear wall interconnected with coupling beams", ***HighTech and Innovation Journal***, Vol. 3, No. 2, (2022), 230-242. doi: 10.28991/HIJ-2022-03-02-010.
20. Mirjavadi, S.S., Mohasel Afshari, B., Shafiei, N., Rabby, S. and Kazemi, M., "Effect of temperature and porosity on the vibration behavior of two-dimensional functionally graded micro-scale timoshenko beam", ***Journal of Vibration and Control***, Vol. 24, No. 18, (2018), 4211-4225. doi: 10.1177/1077546317721871.
21. Şimşek, M., "Buckling of timoshenko beams composed of two-dimensional functionally graded material (2d-fgm) having different boundary conditions", ***Composite Structures***, Vol. 149, (2016), 304-314. doi: 10.1016/j.compstruct.2016.04.034.
22. Timoshenko, S.P., "X. On the transverse vibrations of bars of uniform cross-section", ***The London, Edinburgh, and Dublin Philosophical Magazine and Journal of Science***, Vol. 43, No. 253, (1922), 125-131. doi: 10.1080/14786442208633855.
23. Aydogdu, M. and Taskin, V., "Free vibration analysis of functionally graded beams with simply supported edges", ***Materials & Design***, Vol. 28, No. 5, (2007), 1651-1656. doi: 10.1016/j.matdes.2006.02.007.
24. Simsek, M., "Fundamental frequency analysis of functionally graded beams by using different higher-order beam theories", ***Nuclear Engineering and Design***, Vol. 240, (2010), 697-705. doi: 10.1016/j.nucengdes.2009.12.013.
25. Elmeiche, A., Megueni, A. and Lousdad, A., "Free vibration analysis of functionally graded nanobeams based on different order beam theories using ritz method", ***Periodica Polytechnica Mechanical Engineering***, Vol. 60, No. 4, (2016), 209-219. doi: 10.3311/PPme.8707.

26. Khorshidi, K. and Shabani, Y., "Free vibration analysis of sandwich plates with magnetorheological smart fluid core by using modified shear deformation theory", ***Journal of Science and Technology of Composites***, (2022), doi: 10.22068/jstc.2022.552957.1782.

27. Khorshidi, K., Taheri, M. and Ghasemi, M., "Sensitivity analysis of vibrating laminated composite rec-tangular plates in interaction with inviscid fluid using efast method", ***Mechanics of Advanced Composite Structures***, Vol. 7, No. 2, (2020), 219-231. doi: 10.22075/macs.2020.18605.1224.

28. Khorshidi, K. and Karimi, M., "Analytical approach for thermo-electro-mechanical vibration of piezoelectric nanoplates resting on elastic foundations based on nonlocal theory", ***Mechanics of Advanced Composite Structures***, Vol. 6, No. 2, (2019), 117-129. doi: 10.22075/macs.2019.15518.1156.

29. Ghayesh, M.H., Amabili, M. and Farokhi, H., "Nonlinear forced vibrations of a microbeam based on the strain gradient elasticity theory", ***International Journal of Engineering Science***, Vol. 63, (2013), 52-60. doi: 10.1016/j.ijengsci.2012.12.001.

30. Shabani, Y. and Khorshidi, K., "Free vibration analysis of rectangular doubly curved auxetic-core sandwich panels integrated with cnt-reinforced composite layers using galerkin method", ***Journal of Science and Technology of Composites***, Vol. 8, No. 3, (2022), 1686-1677. doi: 10.22068/jstc.2022.545477.1762.

31. Khorshidi, K. and Fallah, A., "Free vibration analysis of size-dependent, functionally graded, rectangular nano/micro-plates based on modified nonlinear couple stress shear deformation plate theories", ***Mechanics of Advanced Composite Structures***, Vol. 4, No. 2, (2017), doi: 10.22075/MACS.2017.1800.1094.

32. Mohamed, B., Elmeiche, A., Elhennani, A., Kebir, T., El, Z. and zine el abidine, H., "Exact solution for free vibration analysis of fgm beams", ***Revue des Composites et des Matériaux Avancés***, Vol. 30, (2020). doi: 10.18280/rcma.300201.

33. Reddy, J.N. and Robbins, D.H., Jr, "Theories and computational models for composite laminates", ***Applied Mechanics Reviews***, Vol. 47, No. 6, (1994), 147-169. doi: 10.1115/1.3111076.

Persian Abstract

چکیده

در این پژوهش ارتعاش آزاد تیرهای ساندویچی مدرج تابعی دو جهته متخلخل ارائه شده‌است. معادلات حاکم بر تیر به کمک اصل همیلتون استخراج شده و با استفاده از روش گلرکین حل شده‌اند. خواص مواد تیر ساندویچی در راستای ضخامت و طول هر لایه از تیر، با توجه به نسبت‌های حجمی مدرج متغییر می‌باشند. خواص مکانیکی تیر بین آلومینیوم و آلومینیا ،به عنوان فلز و سرامیک، به صورت تدریجی تغییر می‌کنند. ارتعاش آزاد براساس دو تئوری مرتبه بالای برشی جدید که در این پژوهش برای اولین بار ارائه شده‌اند، برای سه مدل متفاوت تیر محاسبه گردیده‌است. نتایج حاصل با تئوری‌های تغییر شکل برشی تیموشنکو، مرتبه اول و پارابولیکی قیاس شده‌اند. علاوه بر این، تاثیر تخلخل، نسبت طول به ضخامت تیر و نسبت‌های حجمی مدرجی در راستای طول و ضخامت برروی فرکانس‌ها بررسی شده‌اند. همچنین، شکل مودهای تیر تحت نسبت‌های حجمی متفاوت براساس تئوری جدید ترسیم گردید. صحت نتایج حاصل از دو تئوری جدید با نتایج دو مقاله با روش‌های حل دقیق و تحلیلی مقایسه گردیده‌است.